ELSEVIER

Surface Science 482–485 (2001) 1406–1412

SURFACE SCIENCE

www.elsevier.nl/locate/susc

Initial stages of Sn adsorption on Si(1 1 1)-(7 × 7)

O. Custance, I. Brihuega, J.M. Gómez-Rodríguez *, A.M. Baró

Departamento de Física de la Materia Condensada, C-III, Universidad Autónoma de Madrid, Cantoblanco, E-28049 Madrid, Spain

Abstract

By means of scanning tunneling microscopy (STM) we have performed a detailed analysis of the initial stages of Sn adsorption on Si(1 1 1)-(7 × 7) at room temperature (RT). At very low coverages ($\Theta \approx 0.01$ ML) single Sn atoms as well as clusters of two Sn atoms can be resolved inside the (7 × 7)-half-cells. According to our STM measurements, single Sn atoms are highly mobile at RT inside the (7 × 7)-half-cells. This thermally activated motion, faster than the scanning speed, results in a characteristic fuzzy appearance of the half-cell. This behavior was first reported for the Pb/Si(1 1 1)-(7 × 7) system and has since then been observed in the initial stages of growth at RT of other adsorbates on Si(1 1 1)-(7 × 7) surfaces. For the Sn/Si(1 1 1)-(7 × 7) system, by combining real-time STM observations with measurements of cluster size distributions we have been able to gain some insight into the mechanisms involved in the first stages of growth. In particular, the differences observed in relation to the Pb/Si(1 1 1)-(7 × 7) are discussed.

Keywords: Scanning tunneling microscopy; Epitaxy; Growth; Surface diffusion; Surface structure, morphology, roughness, and topography; Silicon; Tin

1. Introduction

The fabrication and analysis of nanostructures formed by a few atoms is becoming a subject of increasing interest due to both theoretical and experimental reasons [1]. In particular, the development of more and more complex and small devices is based on the ability to control these structures down to the atomic level. In this sense, the knowledge of the dynamical processes and the local stability of atomic structures on semiconductor surfaces has a fundamental importance [2]. Scanning tunneling microscopy (STM) has proven to be a powerful tool for the analysis at the atomic scale of these processes involved in the initial stages of adsorbate growth on semiconductor surfaces.

Tin or lead deposition on Si(1 1 1) surfaces has received an increasing interest in the last few years. These compounds are known to form an unreactive interface due to their negligible solubility in Si [3]. In the specific case of Sn, previous works were focused on the analysis of high coverage phases obtained on annealed samples [4–13], while less attention has been devoted to the initial stages of Sn chemisorption at room temperature (RT) [14].

In this work a detailed STM analysis of the very initial stages of growth of Sn on Si(1 1 1)-(7 × 7) surfaces at RT is presented. Single Sn atoms as well as pairs of Sn atoms have been resolved for ultra low coverage deposits. Surface diffusion and

* Corresponding author. Tel.: +34-1-3974752; fax: +34-1-3973961.

E-mail address: josem.gomez@uam.es (J.M. Gómez-Rodríguez).

0039-6028/01/$ - see front matter
PII: S0039-6028(01)00732-4

nucleation events have been studied and are discussed with reference to the related system Pb/Si(1 1 1)-(7 × 7) [15–18].

2. Experimental

The experiments were carried out in an ultra-high-vacuum (UHV) system composed of two interconnected UHV chambers. The first one contains a home-made beetle-type STM. The second chamber is equipped with low energy electron diffraction, Auger electron spectroscopy, sample and STM-tip transfer and heating capabilities, several interchangeable evaporation cells, a quartz crystal microbalance and a quadrupole mass spectrometer (QMS). The base pressure of both chambers is below 5×10^{-11} Torr.

Clean reconstructed Si(1 1 1)-7 × 7 surfaces were prepared by flashing the samples (p-type B-doped Si(1 1 1), resistivity = 0.01 Ω cm) at 1150°C, after carefully degassing at 600°C for several hours. The samples were then slowly cooled down to RT. 0.01 Sn monolayer (ML) were deposited onto the Si(1 1 1)-7 × 7 surface at RT. 1 ML is defined as the density of the Si atoms on the Si(1 1 1) surface: 7.8×10^{14} atoms/cm^2. Sn was evaporated from a home-built evaporation cell consisting of a Ta boat heated by electron bombardment from a W filament. During the evaporation the residual pressure in the UHV chamber remained below 1×10^{-10} Torr and the evaporation rate (typically 0.05 ML/min) was monitored by a quartz crystal microbalance and a QMS.

STM data were acquired with a fully automated workstation which incorporates digital feedback control based on digital signal processor technology [19]. STM was operated in the constant current mode with variable sample voltages between −2 and +2 V and typical tunnel currents of 100–200 pA.

3. Results

Fig. 1 shows a typical large scale (50 × 50 nm^2) occupied state STM image of Sn/Si(1 1 1)-(7 × 7) at 0.01 ML. At this extremely low coverage, the surface retains the original (7 × 7) reconstruction. The deposited Sn appears as bright features at both polarities and small metal clusters of Sn adatoms adsorbed on the Si surface are clearly observed on some halves of the (7 × 7) unit cells. Further insight can be gained when zooming to higher magnification as shown in Fig. 2. Simultaneously measured occupied and unoccupied-state STM images are presented in order to distinguish the faulted and unfaulted halves of the 7 × 7 unit cell. Three kind of protrusions related to Sn adsorption on the Si(1 1 1)-(7 × 7) can be resolved at this coverage:

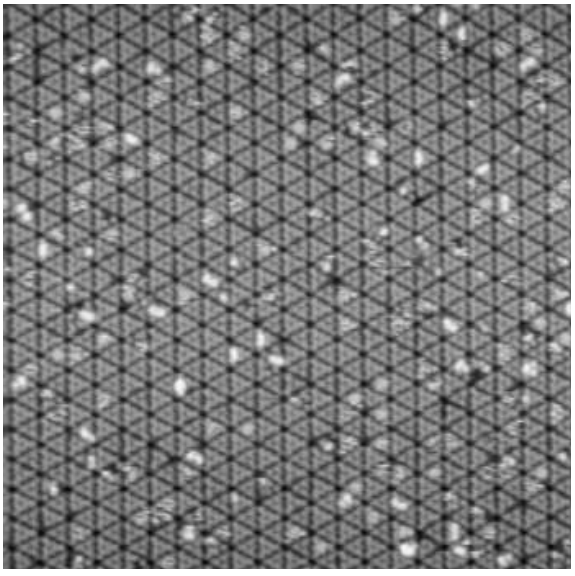

Fig. 1. Occupied state STM image measured on Sn/Si(1 1 1)-(7 × 7) at 0.01 ML coverage. The scanning area is 50 × 50 nm^2. The sample voltage is −1.5 V and the tunnel current is 200 pA.

1. Some (7 × 7)-half-cells present a rather fuzzy or noisy aspect (labeled with S in Fig. 2).
2. Other half-cells show two well-defined protrusions that can be clearly resolved in both occupied and unoccupied-state images (labeled P in Fig. 2).
3. Finally, some half-cells are occupied by oblong protrusions (labeled P* in Fig. 2). These protrusions present two maxima separated by ≈4.7 Å. Notice that this value is much smaller than the one found on the P-type protrusions (≈7.7 Å).

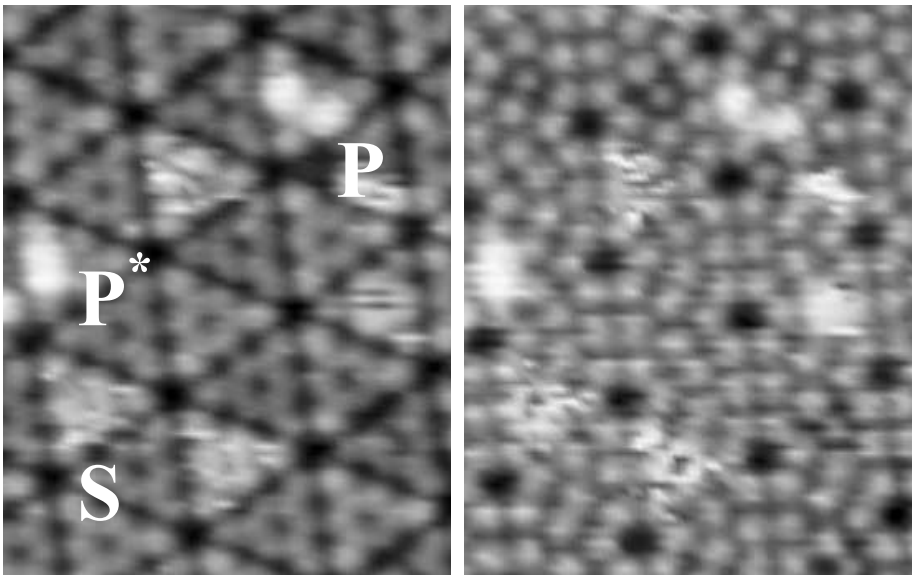

Fig. 2. Simultaneously measured occupied (a) and unoccupied-state (b) STM images of Sn/Si(1 1 1)-(7×7). The labels identify single Sn adatoms (S) and pairs (P,P*) as discussed in the main text. The sample voltages are (a) -2 V and (b) $+2$ V and the tunneling current is 100 pA.

By similarity to the Pb/Si(1 1 1)-(7×7) system [15–17] one could tentatively ascribe the first two kinds of structures to the adsorption of one single Sn adatom (S) inside the (7×7)-half-cell and to the adsorption of a pair of two Sn atoms (P), respectively. The noisy aspect of the half-cells containing an S-type protrusion would be the result of the fast movement of a single atom among different adsorption sites inside the half-cell at much faster rates than the STM scanning speed. This comparison, however, does not shed any light on the possible origin of the P*-type protrusions, as this kind of features is not observed in the case of Pb on Si(1 1 1)-(7×7) at RT.

More information can be gained on the interpretation of these three kinds of protrusions by measuring "STM movies", i.e. series of successive STM images acquired over the same surface area for long periods of time. Fig. 3 presents two frames extracted from a STM movie. In the time elapsed between the acquisition of these frames, two S-type protrusions which were observed in two neighboring half-cells have become one P-type protrusions (indicated by a white arrow in Fig. 3). This observation is consistent with the assumption that S-type protrusions correspond to single Sn adatoms and P-type protrusions to a pair of Sn adatoms. Thus, clusters of two atoms could be formed as the result of single atom diffusion processes leading to Sn pair formation.

The uncertain origin of P*-type protrusions was investigated by measuring long series of STM movies (2–3 h) on the same areas. Fig. 4 shows frames extracted from two STM movies measured simultaneously at both sample polarities. These STM images suggest a close relationship between P-type and P*-type protrusions. The P-type pair observed in Fig. 4(a) and (b) transforms into a P*-type protrusion in Fig. 4(c) and (d). Transformations of P* to P-type protrusions were also observed (not shown). This reversibility of P $\Longleftrightarrow$ P* transformations allows us to identify the P*-type protrusions with the adsorption of a pair of Sn adatoms inside the (7×7)-half-cell. Thus, both P and P*-type protrusions correspond to the adsorption of a pair of Sn adatoms though the

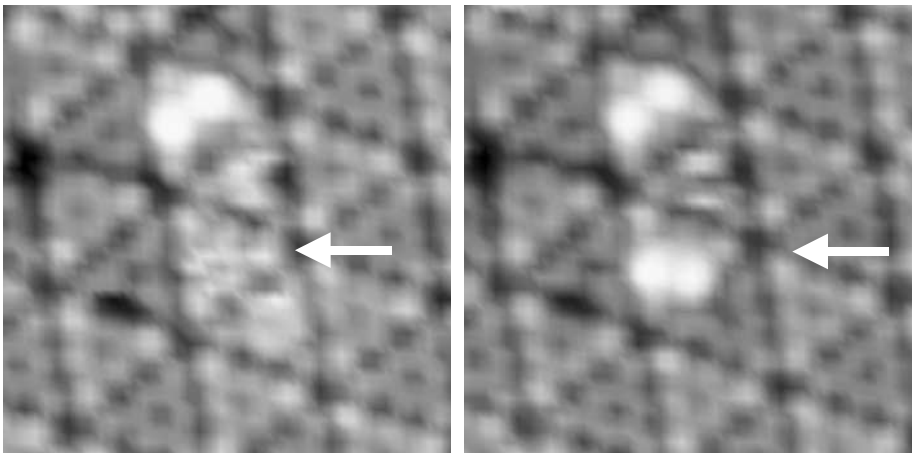

Fig. 3. Frames extracted from an STM movie showing the diffusion of a single Sn adatom to a neighboring Si(1 1 1)-(7 × 7) half-cell and the formation of a pair. Time between frames: 164 s. Image size: 8.2 × 8.2 nm^2. Tunneling conditions: $V = -1.5$ V, $I = 200$ pA.

adsorption state or geometry of each structure is probably different.

In order to discard a direct influence of the STM scanning process on the dynamic events described in the present work, we have checked that single atom jump to neighbor half-cells and $P \Longleftrightarrow P^*$ transformation events do happen at both sample bias polarities, with different tunneling currents and scanning speeds.

4. Discussion

The results shown in the precedent section depict the following scenario for the growth of the Sn/Si(1 1 1)-(7 × 7) system at RT in the very initial stages. Sn atoms from the vapor phase are adsorbed on the Si surface. The atoms are confined within the (7 × 7)-half-cell. There is a probability that two Sn atoms fall into the same half-cell or into neighboring half-cells in which case they react to form a pair of adatoms.

Single Sn adatoms, as revealed by the STM measurements, are highly mobile at RT inside the (7 × 7)-half-cells. Their thermally activated motion, which is faster than the scanning speed, results in the characteristic fuzzy appearance of the half-cell. This behavior was first reported for the Pb/Si(1 1 1)-(7 × 7) interface [15–17] and later for Tl [20], Si [21] and Y [22] on Si(1 1 1)-(7 × 7) surfaces. Moreover, this behavior was also observed for the adsorption of Pb on another complex metastable reconstruction of the Si(1 1 1) surface, the (5 × 5) reconstruction [18], which obeys to the same Dimer–Adatom-Stacking Fault model as the (7 × 7)-reconstruction. All these experimental findings are consistent with the "intermittent diffusion" image proposed by Cho and Kaxiras [23,24] for the adsorption and diffusion of extra adatoms on reconstructed Si(1 1 1) surfaces. In accordance with their density-functional total energy calculations, the diffusion path is characterized by the existence of "basins of attraction" inside the (7 × 7)-half-cells. This could be the case for the Sn single adatoms. Sn atoms remain, at RT, almost completely trapped inside the (7 × 7)-half-cells but perform thermally activated jumps between different basins of attraction separated by low energy barriers. Lower temperature measurements are needed to resolve single-atom jumping within the half-cells for the Sn/Si(1 1 1)-(7 × 7) system. Very recent results obtained for Pb/Si-(1 1 1)-(7 × 7) at 60 K with variable-temperature STM [25] have revealed the existence of three basins of attraction inside the (7 × 7)-half-cells. Based on the similarity of the two systems, such a

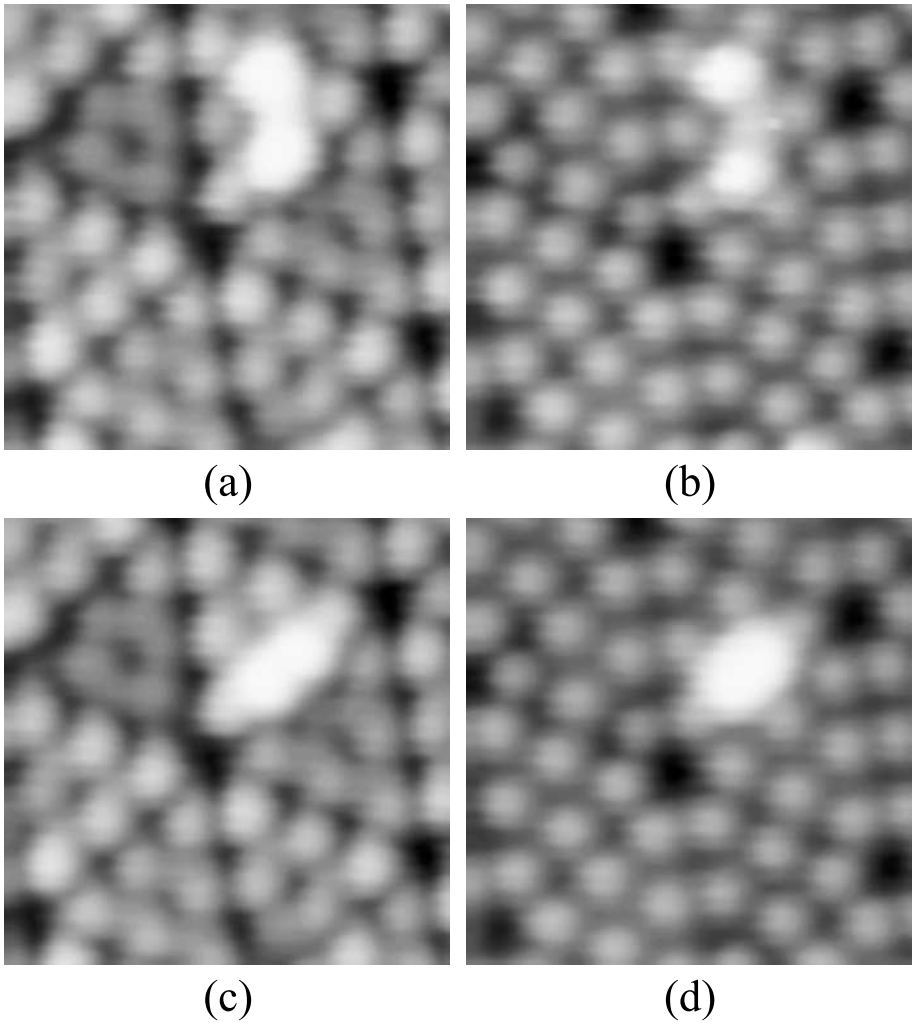

Fig. 4. Frames extracted from two simultaneously measured STM movies at (a, c) −1.5 V and (b, d) +1.5 V sample voltages. The sequence illustrates the transformation of a P pair into a P^* pair (see text). The time between frames (a, b) and (c, d) is 1640 s. The image size is 5.4×5.4 nm^2. The tunnel current is 200 pA.

behavior should be extensible to the Sn/Si(1 1 1)-(7×7) interface.

As shown in Fig. 3, single Sn atoms can jump at RT to the nearest neighbor half-cells where other single Sn atoms are trapped, to form a pair. However, no jumps of Sn single adatoms have been detected to nearest neighbor half-cells free of Sn adatom in spite of long periods of observation time (2–3 h) of large surface areas (typically 50×50 nm^2). This is in contrast to the Pb/Si(1 1 1)-(7×7) system where Pb single atom diffusion into empty nearest-neighbor half-cells was detected at RT [15]. This observation indicates a higher energy barrier for Sn adatoms. Moreover, this barrier could be lowered by the presence of Sn adatoms in the nearest neighbor half-cells. A long range attractive interaction would exist to favor the formation of Sn pair. This fact can be analyzed by calculating the Sn cluster size distribution using a simple model already described in Ref. [15]. According to this model, the cluster-size distribution should obey a Poisson distribution in the form:

$$C_n = (sn!)^{-1}(s\theta)^n \exp(-s\theta) \quad (1)$$

where C_n is the average number per half-cell of clusters formed by n Sn atoms, θ is the coverage in half-cell units, i.e. the average number of Sn atoms per half-cell and s is an effective capture area, defined as the number of half-cells which contribute to the formation of a cluster of size n (i.e., $s = 1$ for capture by direct impingement from the vapor phase and $s = 4$ for capture by atom jumps from the three nearest neighbor half-cells on the half-cell of the cluster).

Fig. 5 shows the initial cluster-size distribution experimentally obtained from large sets of STM data measured some minutes after the deposits were performed. Also shown are the cluster size distributions obtained from Eq. (1) for two physically reasonable values of s, i.e. $s = 1$ and $s = 4$. None of the two theoretical values fits properly the experimental distribution. This is again in contrast to the Pb/Si(1 1 1)-(7×7) where the model with $s = 4$ gave a much better account for the experimental results. This probably means that, although some interaction does exist for Sn adatoms in nearest-neighbor half-cells, lowering the number of half-cells occupied by a single atom by increasing the number of those occupied by pairs (P and P*), the lowering of the energy barrier that it produces is not so important as in the Pb/Si(1 1 1)-(7×7) case. Moreover, as discussed in Ref. [15], in the simplified model from which Eq. (1) is derived, it is considered that clusters of size n will capture instantaneously all atoms from the incident beam that land on the surface inside its capture area. This rough approximation of instantaneous capture was supported by two facts in the case of Pb/Si(1 1 1)-(7×7):

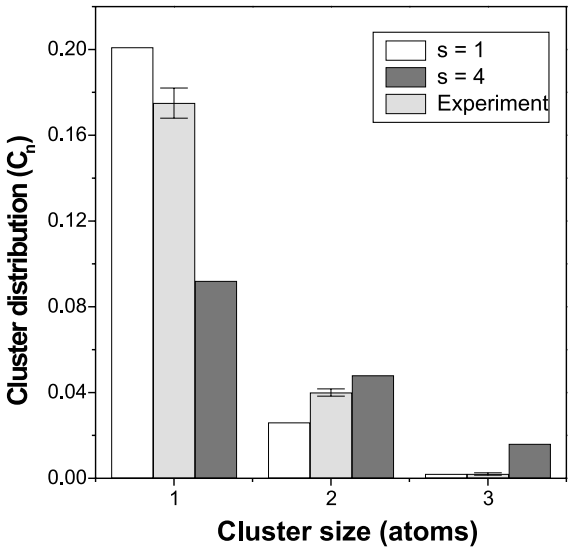

Fig. 5. Initial cluster-size distributions of Sn on Si(1 1 1)-(7×7) at ≈0.01 ML (θ in Eq. (1) was measured from the STM images, resulting in a value of 0.26).

1. Pb monomers diffuse at RT at extremely low rates ($\sim 2 \times 10^{-5}$ s^{-1}, see Fig. 4 in Ref. [15]) to nearest neighbor half-cells which are not occupied by other Pb cluster.
2. In contrast, the formation of a pair from two monomers in nearest neighbor half-cells takes place always in a time scale of a few seconds.

For the Sn/Si(1 1 1)-(7×7) system the first of these observations still holds. The second one, however, is not so well justified. In fact, the formation of pairs from two single adatoms in adjacent half-cells takes a time in the range of some minutes, i.e., much longer than in the Pb/Si(1 1 1)-(7×7) case. This difference is closely related to the present discrepancy between the experimental and calculated distributions and shows that, due to the differences between both systems, such simple model cannot accurately account for the observations on the Sn/Si(1 1 1)-(7×7) interface.

A final interesting issue to address is the different occupancy probability of Sn clusters on the two not equivalent halves of the (7×7)-unit cell, faulted (F) and unfaulted (U). According to the present experiments, the ratio for single Sn adatoms adsorbed on F and U is ≈1, whereas this ratio for Sn pairs P and P* is ≈1.5. This latter value is close to that reported by Lin et al. [14] for Sn/Si(1 1 1)-(7×7) on higher coverage deposits. As stated by these authors the difference in electronic structures between the two in-equivalent halves is the origin of preferential occupation of F by Sn clusters [26,27]. The situation for single Sn atoms is different, however, since there is not a preferential occupation. This can be understood in terms of the low probability for a single Sn adatom

to jump to nearest neighbor half-cells at RT. Thus, the asymmetry in the occupancy of faulted vs. unfaulted halves of the (7×7) reconstruction for Sn pairs must come from the joining of the single adatoms on adjacent halves to form a pair.

5. Conclusions

The initial stages of Sn chemisorption on Si(1 1 1)-(7×7) surfaces at RT have been studied by means of STM. Highly mobile Sn single adatoms almost trapped inside the (7×7)-half-cells have been detected and the nucleation of pairs of Sn adatoms from two single Sn atoms has been resolved in real time. From the analysis of cluster size distributions at very low Sn coverages and the observation of single adatom jumping to nearest neighbor half-cells already occupied by another single adatom, the existence of an attractive interaction between neighbor Sn adatoms has been proposed.

References

[1] D.M. Eigler, E.K. Schweizer, Nature 344 (1990) 524.
[2] E. Kaxiras, Thin Solid Films 272 (1996) 386.
[3] A. Cricenti, M. Göthelid, G. Le Lay, Surf. Sci. 382 (1997) 182.
[4] T. Kinoshita, H. Ohta, Y. Enta, Y. Yaegashi, S. Suzuki, S. Kono, J. Phys. Soc. Jpn. 56 (1987) 4015.
[5] J. Nogami, S.-i. Park, C.F. Quate, J. Vac. Sci. Technol. A 7 (1989) 1919.
[6] J.A. Kubby, Y.R. Wang, W.J. Greene, Phys. Rev. Lett. 65 (1990) 2165.
[7] C. Törnevik, M. Hammar, N.G. Nilsson, S.F. Flodström, Phys. Rev. B 44 (1991) 13144.
[8] C. Törnevik, M. Göthlied, M. Hammar, U.O. Karlsson, N.G. Nilsson, S.A. Flodström, C. Wigren, M. Östling, Surf. Sci. 314 (1994) 179.
[9] M. Göthelid, M. Björkqvist, T.M. Grehk, G. Le Lay, U.O. Karlsson, Phys. Rev. B 52 (1995) R14352.
[10] D.T. Wang, N. Esser, M. Cardona, J. Zegenhagen, Surf. Sci. 343 (1995) 31.
[11] X.F. Lin, I. Chizhov, H.A. Mai, R.F. Willis, Appl. Surf. Sci. 104–105 (1996) 223.
[12] A.H. Levermann, et al., Appl. Surf. Sci. 104–105 (1996) 124.
[13] H.T. Anyele, C.L. Griffiths, A.A. Cafolla, C.C. Matthai, R.H. Williams, Appl. Surf. Sci. 123–124 (1998) 480.
[14] X.F. Lin, I. Chizhov, H.A. Mai, R.F. Willis, Surf. Sci. 366 (1996) 51.
[15] J.M. Gómez-Rodríguez, J.J. Sáenz, A.M. Baró, J.-Y. Veuillen, R.C. Cinti, Phys. Rev. Lett. 76 (1996) 799.
[16] J.M. Gómez-Rodríguez, J.-Y. Veuillen, R.C. Cinti, J. Vac. Sci. Technol. B 14 (1996) 1005.
[17] J.M. Gómez-Rodríguez, J.-Y. Veuillen, R.C. Cinti, Surf. Rev. Lett. 4 (1997) 335.
[18] J.-Y. Veuillen, J.M. Gómez-Rodríguez, A.M. Baró, R.C. Cinti, Surf. Sci. 377–379 (1997) 847.
[19] Nanotec Electrónica S.L. http://www.nanotec.es.
[20] L. Vitali, M.G. Ramsey, F.P. Netzer, Phys. Rev. Lett. 83 (1999) 316.
[21] Y. Sato, S. Kitamura, M. Iwatsuki, Surf. Sci. 445 (2000) 130.
[22] C. Polop, J.L. Sacedón, J.A. Martín-Gago, Surf. Sci., in press.
[23] K. Cho, E. Kaxiras, Europhys. Lett. 39 (1997) 287.
[24] K. Cho, E. Kaxiras, Surf. Sci. 396 (1998) L261.
[25] O. Custance, J.M. Gómez-Rodríguez, A.M. Baró, L. Juré, P. Mallet, J.-Y. Veuillen, in press.
[26] St. Tosh, H. Neddermeyer, Phys. Rev. Lett. 61 (1988) 349.
[27] U.K. Köhler, J.E. Demuth, R.J. Hamers, Phys. Rev. Lett. 60 (1988) 2499.